

## An Experimental Investigation of Structured Roughness on Heat Transfer during Single-Phase Liquid Flow at Microscale

Ting-Yu Lin and Satish G. Kandlikar \*

\* Corresponding author: Tel.: 585.475.6728; Fax: 585.475.7710; Email: sgkeme@rit.edu  
Mechanical Engineering Department, Rochester Institute of Technology, USA

### Abstract

The effect of structured roughness on the heat transfer of water flowing through minichannels was experimentally investigated in this study. The test channels were formed by two stainless steel plates, 4 mm thick, 12.7 mm tall, and 94.6 mm in length. The surfaces of the plates forming the channel walls were machined with structured roughness elements with height ranging from 18  $\mu\text{m}$  to 96  $\mu\text{m}$ , and pitch ranging from 250  $\mu\text{m}$  to 400  $\mu\text{m}$ . The hydraulic diameter of the channels range from 0.71 mm to 1.87 mm. After accounting for the heat loss from the edges and end sections, the heat transfer coefficient for smooth channels was calculated. The coefficient was found to be in good agreement with the conventional correlations in the laminar entry region and laminar fully developed region. Convective heat transfer was found to be enhanced by the roughness. In the ranges of tested parameters, the roughness element pitch was found to have almost no effect, while the heat transfer coefficient was significantly enhanced by increasing the roughness element height. An earlier transition from laminar to turbulent flow was observed with increasing relative roughness. Comparing with inserts, the highest relative roughness element provided the highest thermal performance factor in the Reynolds number in the range from about 400 to 2800.

**Keywords:** Roughness, Microscale Heat transfer, Structured Roughness, minichannels

### 1. Introduction

Heat transfer in microscale passages is of great interest due to its application in micro heat exchangers, fuel cells, biomedical devices, etc. These passages can be formed by generating grooves on a substrate through CNC/MEMS technology and then covering them with a top cover. A number of earlier investigations on laminar flow at the microscale reported a significant departure from conventional heat transfer predictions [1-6], while the more recent literature revealed heat transfer data of liquid flow that is in agreement with conventional theory [7-10]. Data reduction, experimental uncertainty, and incorrect boundary conditions were found to be the major reasons in earlier investigations [11-16] showing disagreement. Some of the experimental issues were discussed in the

literature: Celata et al. [17] revealed the effect of inaccurate measurement of tube diameters on friction factors. Using a 40X microscope, the diameter was measured as 84.7  $\mu\text{m}$ , and the resulting friction factor was significantly higher than the prediction. While using a 400X microscope, the diameter of the same tube was found to be 80.0  $\mu\text{m}$  and the data was predicted very well by the conventional correlation. Li et al. [18] indicated that Wu and Little [1] did not measure the wall roughness directly, but obtained the value of equivalent sand roughness from their  $f Re-Re$  chart. Mala and Li [19] relied on the manufacturers data for the values of relative roughness, and used the concept of roughness-viscosity to correlate their data. Herwig and Hausner [20] indicated that axial heat conduction was the major reason for the discrepancy in the experimental

data of Tso and Mahulikar [21].

Many experimental data reported in the literature indicate a lower value of fully developed Nusselt number in laminar flow, with a decreasing trend at lower Reynolds numbers [2, 3, 5, 6, 22-24]. The reason for lower heat transfer coefficients as compared to the conventional correlation could be attributed to the axial conduction effect. Lin and Kandlikar [2011] [25] proposed a model to quantitatively estimate the axial conduction effect. From their model, the axial conduction effect is not negligible for fluid flow in channels with the following characteristics: large wall thickness, small diameter, high wall thermal conductivity, low fluid conductivity, and low Re. On the other hand, some data exhibited a higher heat transfer coefficient, which can be mainly attributed to the roughness effect [1, 10, 26-30].

Heat transfer enhancement in both laminar and turbulent flows has been an area of great interest for quite a long time [31]. In macroscale laminar flow, some of the enhancement techniques receiving renewed interest are: twisted tubes [32, 33], porous materials [34], and coiled wires [35]. In turbulent flow, enhanced structure on channel internal walls was investigated and found to enhance heat transfer. There is very limited data available for studying the systematic effect of enhancement techniques on heat transfer and pressure drop.

Friction factors in mini and micro scale rough channels were systematically investigated by Kandlikar et al. [36-39]. The effect of the roughness element height, pitch, and relative roughness were studied in detail. A model was

proposed to predict the early transition from laminar to turbulent flow due to roughness effects [38, 39]. However, there are very few studies in the literature that systematically investigate the effect of roughness on heat transfer in microchannels [27].

The present work is aimed at systematically investigating the effects of structured roughness elements on heat transfer at the microscale. The structure roughness parameters investigated include: roughness element pitch,  $\lambda$ , height, H, and the relative roughness H/D.

## 2. Experimental Setup

Figure 1 shows a schematic of the test system. Degassed, distilled water is circulated through the system by a micro pump. The water is supplied from a reservoir and is conditioned through a heat exchanger with an outside loop cooled by a chiller. The water then flows through a bank of flow meters, which includes two flow meters in parallel with working ranges of 10-100 ml/min and 60-1000 ml/min respectively. The water exits the test section and is returned to the reservoir.

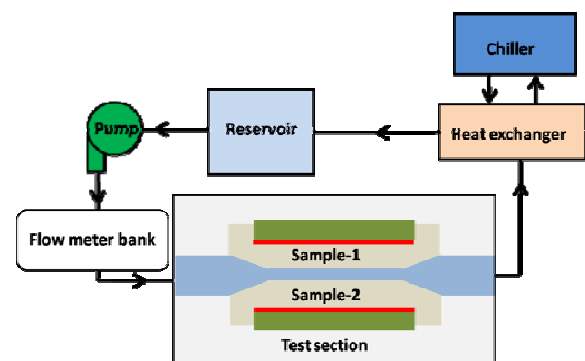


Fig. 1. Schematic drawing of experimental system

In the present study, the flow channel was formed by two thin stainless steel sections. The advantages of using stainless steel walls are: (i) Reasonably high thermal conductivity to transfer heat from the heaters to the liquid, (ii) Higher strength to withstand high compression force required to prevent leakage, and (iii) Low enough thermal conductivity to avoid severe effects due to axial conduction.

The structured roughness elements on the stainless steel walls were generated by CNC machining. The pitch to height ratio of the structured roughness elements has been identified as a key parameter affecting fluid flow and heat transfer [40]. In this study the sinusoidal roughness surfaces are employed with pitch to height ratios ranging from 2.6 to 13.9. The actual fabricated surface profiles are obtained from a Confocal Laser Scanning Microscope. The surface profile of the roughness elements is shown in Fig. 2. Table 1 lists the roughness element pitches,  $\lambda$ , roughness element heights,  $H$ , and hydraulic diameters investigated in this work.

The roughness surface profile has a sinusoidal shape that can be described by the following equation:

$$y(x) = H[\cos(\frac{\pi}{\lambda}x)]^P \quad (1)$$

where  $P$  is the power on the cosine which controls the slope of the peaks. The values of  $P$  for channels **B**, **C**, **D** and **E** in Table 1 are 4, 12, 32 and 4, respectively.

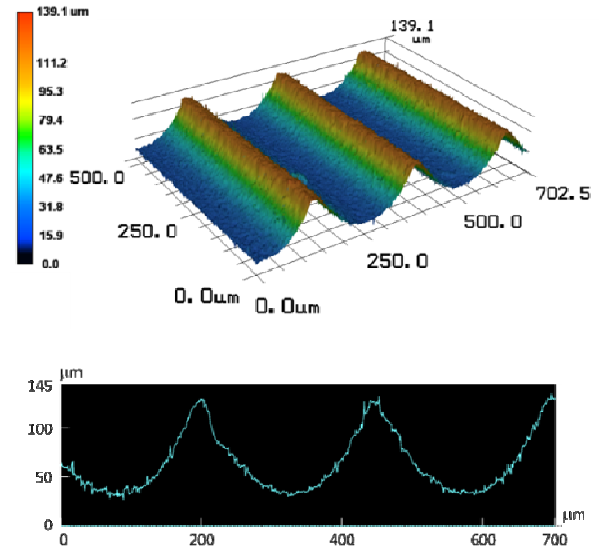


Fig. 2. Test sample surface profiles measured by Confocal Laser Scanning Microscope (a) 3 dimensional (b) 2 dimensional ( $\lambda=250 \mu\text{m}$ ,  $H=96.3 \mu\text{m}$ )

Table 1 Surface geometry of test sections

Channel	A-1	A-2	B-1	B-2	C-1	C-2
$\lambda$ ( $\mu\text{m}$ )	Smooth		250		250	
$H$ ( $\mu\text{m}$ )	Smooth		96.3		32	
$\lambda/H$	Smooth		2.6		7.8	
$b$ ( $\mu\text{m}$ )	500	700	450	1011	382	908
$D_h$ (mm)	0.96	1.33	0.87	1.87	0.74	1.69
$H/b$ (%)	0	0	21.4	9.5	8.4	3.5
$H/D_h$ (%)	0	0	11.1	5.1	4.3	1.9
Channel	D-1	D-2	E-1	E-2		
$\lambda$ ( $\mu\text{m}$ )	400		250			
$H$ ( $\mu\text{m}$ )	37.7		18			
$\lambda/H$	10.6		13.9			
$b$ ( $\mu\text{m}$ )	401	981	366	912		
$D_h$ (mm)	0.78	1.82	0.71	1.70		
$H/b$ (%)	9.4	3.8	4.9	2.0		
$H/D_h$ (%)	4.8	2.1	2.5	1.1		

## 2.1 Effect of axial conduction

The effect of axial heat conduction was

investigated by Lin and Kandlikar [2011] [25] and Maranzana et al. [41] and Guo and Li [12]. Figure 3 shows a schematic of a tube section experiencing axial conduction in the fully developed flow region. Under constant heat flux heating, the wall temperature is higher in the flow downstream and hence heat is transferred from downstream to upstream by conduction in the wall. Without considering axial conduction, the heat transfer rate to the fluid in the region up to the section under consideration is  $q_{conv} = q''A_h$ , while with the axial conduction the heat transfer rate is  $q_{conv} = q''A_h + q_{cond}$ , where  $A_h$  and  $q_{cond}$  are the convective heat transfer area and the axial conduction heat transfer rate. The temperature  $T_f$  is higher due to the axial conduction effect as the heat conducted in the wall enters the fluid prior to that section.

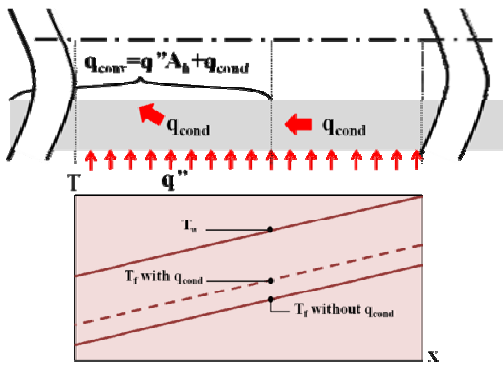


Fig. 3. Schematic drawing of axial conduction effect to fluid temperature

The ratio of axial conduction to convective heat transfer rates,  $q_{cond}/q_{conv}$ , was defined as Cond and M parameter [12, 41]. The axial conduction effects are negligible when M is less than 1% [41]. Based on the test section of the present study, with  $Re > 70$  the M parameter is less than 1% and the axial conduction effects are negligible. In a recent work, Lin

and Kandlikar [25] proposed a model to estimate the axial conduction effect given by

$$\frac{Nu_{k0}}{Nu_{th}} = \frac{1}{1 + 4 \frac{k_s A_{h,s}}{k_f A_f} \frac{Nu_{th}}{(RePr)^2}} \quad (2)$$

where  $Nu_{th}$  is the theoretical Nu, and  $Nu_{k0}$  is without considering axial conduction,  $k_s$  and  $k_f$  are the thermal conductivity of the channel wall and the fluid respectively.  $A_{h,s}$  is the cross-sectional area of the channel wall, and  $A_f$  is the cross-sectional area for the fluid flow in the channel. A value of  $Nu_{k0}/Nu_{th}$  equal to 1 means that the axial conduction has no effect. The lower the  $Nu_{k0}/Nu_{th}$  value, the higher the axial conduction effect. In the present study the values of  $Nu_{k0}/Nu_{th}$  are found to be around 0.99 for Re higher than 300, and the effect of axial heat conduction is therefore negligible.

### 3. Data reduction

The test section is heated with electric heaters to provide a constant heat flux boundary condition. In order to calculate the local heat transfer coefficient, the wall temperature at eleven locations, and the inlet and outlet fluid temperatures were measured. The local fluid temperature was calculated from the inlet and outlet fluid temperatures given by:

$$T_{f,x} = (T_{f,o} - T_{f,i}) \frac{L_{h,x}}{L_{h,All}} \quad (3)$$

where  $L_{h,x}$  is the distance from the inlet section, and  $L_{h,All}$  is the total heated length. Local fluid temperatures are then used to calculate the local Prandtl number, viscosity, and thermal conductivity. The heat supplied to the fluid is then given by:

$$q_{conv} = \dot{m}c_p(T_{f,o} - T_{f,i}) \quad (4)$$

where  $\dot{m}$ ,  $c_p$ ,  $T_{f,o}$  and  $T_{f,i}$  are mass flow rate, heat capacity, and outlet and inlet fluid temperatures, respectively. The total measured input power,  $q_{mea}$ , is obtained from the voltage and current for the power supply:

$$q_{mea} = I \times V \quad (5)$$

where  $I$  and  $V$  are current and voltage respectively. A separate experiment was performed to calculate the heat loss in each individual location. The average heat flux is calculated from the following equation:

$$q''_{avg} = \frac{q_{mea} - q_{loss}}{A_{h,f}} \quad (6)$$

where  $q_{loss}$  is the heat loss from the channel to the surrounding, and  $A_{h,f}$  is the heat transfer area of the channel. The local heat transfer coefficient is calculated as follows

$$h_x = \frac{q''_{avg}}{T_{w,x} - T_{f,x}} \quad (7)$$

where  $T_{w,x}$  and  $T_{f,x}$  are the local wall and fluid temperatures.  $T_{w,x}$  is measured from the thermocouple. The local Nusselt number  $Nu_x$  is calculated as

$$Nu_x = \frac{h_x D_h}{k_{f,x}} \quad (8)$$

where  $D_h$  is the hydraulic diameter.  $D_h$  is calculated as

$$D_h = \frac{4ab}{2(a+b)} \quad (9)$$

where  $a$  is the width of the channel and  $b$  is the gap distance.

## 4. Results

### 4.1 Experimental data validation with smooth channel

In order to estimate the heat loss, a separate controlled experiment was conducted. The channel plate was heated by a power supply without any fluid flow. The heat supplied was lost by conduction through both the assembly parts and the insulation by natural convection to the surroundings. Since the heat losses were predominantly through the end regions, only the data in the central region is used in the present study.

Figure 4 shows the calculated  $Nu$  in smooth channels plotted as a function of  $1/Gz$  for the data taken only in the central region, where  $1/Gz$  is defined as  $1/Gz = (L_{h,x}/D_h)/(RePr)$ . The following correlation validated by Harms et al. [42] for thermally developing flow in a smooth rectangular channel is also plotted to compare with the present data.

$$Nu = 8.24 - 16.8\alpha + 25.4\alpha^2 - 20.4\alpha^3 + 8.7\alpha^4, \quad 1/Gz \geq 0.1 \quad (10a)$$

$$Nu = 3.35(1/Gz)^{-0.130}\alpha^{-0.120}Pr^{-0.038}, \quad 0.013 \leq 1/Gz < 0.1 \quad (10b)$$

$$Nu = 1.87(1/Gz)^{-0.300}\alpha^{-0.056}Pr^{-0.036}, \quad 0.005 \leq 1/Gz < 0.013 \quad (10c)$$

For laminar fully developed flow in a channel of aspect ratio  $\alpha$ , the Nusselt number is given by:

$$Nu = 8.235(1 - 2.0421\alpha + 3.0853\alpha^2 - 2.4765\alpha^3 + 1.0578\alpha^4 - 0.1861\alpha^5) \quad (11)$$

It is seen from Fig. 4 that the conventional correlations for smooth channels are able to predict the data well. However, in the developing region, larger discrepancies are found. One of the factors causing larger errors may be due to the fact that the conventional correlation for laminar developing flow in

rectangular channels with a high aspect ratio is not as reliable as that for circular tubes.

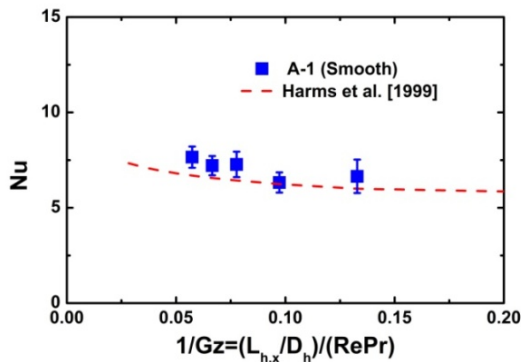


Fig. 4 Comparison of experimental Nu in the center region to the prediction of conventional correlation

#### 4.2 Roughness effects on laminar flow heat transfer

Water flow in rough channels was tested to investigate the effects of roughness on heat transfer. The effects on pressure drop are reported in a separate publication by Wagner and Kandlikar [40]. The surface roughness element structure details are given in Table 1. Channels **B-1**, **B-2**, **C-1**, **C-2**, **E-1** and **E-2** have the same roughness element pitch  $\lambda=250 \mu\text{m}$ , and channels **C-1**, **C-2**, **D-1** and **D-2** have the similar roughness element height  $H$  of about  $35 \mu\text{m}$ . Each roughness element is tested with two different gaps resulting in two different hydraulic diameters.

Figure 5 shows the experimental Nu of rough channel **D-2** normalized by laminar developing flow correlation  $Nu_{th,plain}$  as a function of Re.  $Nu_{th,plain}$  is the theoretical Nu derived from the plain channel equation, Eq. (10). Roughness element **D-2** has  $\lambda=400 \mu\text{m}$ ,  $H=37.7 \mu\text{m}$ , and a hydraulic diameter of 1.76

mm as shown in Table 1. The Nu data for **D-2** is significantly above the prediction from the conventional developing flow correlation for a smooth channel. In developing flow, Nu is a function of Re and increases as Re increases. In Fig. 5,  $Nu/Nu_{th,plain}$  is independent of Re which implies that the slopes of the experimental data and the theoretical values are identical. As mentioned in the previous section, the data were taken in the central region of the channel. The heating length from the flow entrance location  $L_{h,x}$  is about 50 mm, while the thermal fully developed length is about 330 mm at  $Re=1000$ . The experimental data and the theoretical values both depend on Re, while their ratio  $Nu/Nu_{th,plain}$  is seen to be independent of Re.

Amon and Mikic [43] numerically investigated flow patterns and heat transfer in slotted channel flow. Their numerical work indicated that recirculating vortices are generated behind the slot. These vortices are detrimental to heat transfer, but under certain conditions, an oscillatory separated flow was formed resulting in heat transfer enhancement. Dharaiya and Kandlikar [44] numerically investigated the effect of roughness on heat transfer for water flow in the rough channel with the same roughness element structure and channel geometries in the present study. The roughness elements present a series of slots. They found that there are no recirculating vortices generated over the pitch of the roughness elements because of the smooth profile.

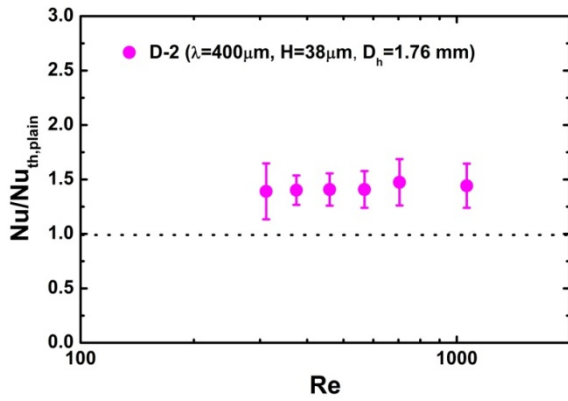


Fig. 5 Comparison of Nu of rough channel (Channel **D-2**) normalized by theoretical developing flow heat transfer correlation

#### 4.3 Effect of roughness element pitch on heat transfer

To study the effects of  $\lambda$ , heat transfer data for **C-2** and **D-2** are plotted in Fig. 6 for comparison. Both surfaces have similar roughness elements with  $H \sim 35 \mu\text{m}$  and  $D_h \sim 1.7 \text{ mm}$ , but with different pitches of  $\lambda=250 \mu\text{m}$  for **C-2** and  $\lambda=400 \mu\text{m}$  for **D-2**. The  $\lambda/H$  ratios for **C-2** and **D-2** are 7.8 and 10.6 respectively. Since the aspect ratio of the two channels are the same,  $Nu_{th,plain}$  is the same for the two data sets. As shown in Fig. 6,  $Nu/Nu_{th,plain}$  is significantly higher than 1 for both data sets.

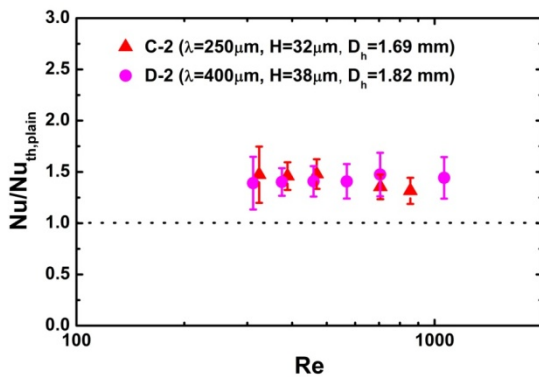


Fig. 6 The effect of roughness element pitch to heat transfer enhancement in channels

By comparing the two data sets, it is found that there is no significant effect of pitch on heat transfer in the ranges of the parameters investigated in the present study.

The effect of roughness on heat transfer under fully developed flow conditions is shown in Fig. 7.

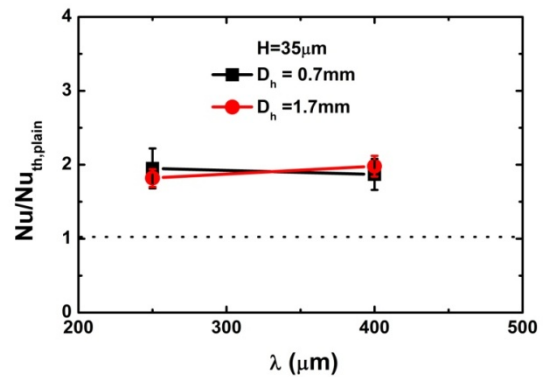


Fig. 7 The effect of roughness element pitch for a roughness height about  $35 \mu\text{m}$

The experimental Nusselt number values are normalized by the theoretical Nusselt number for fully developed laminar flow in a smooth channel. The ratio  $Nu/Nu_{th,plain}$  is plotted as a function of  $\lambda$  for  $H$  around  $35 \mu\text{m}$ . Data sets with the same roughness structure but different hydraulic diameters were also plotted. The rough channels show enhanced performance over a smooth channel, but the effect of  $\lambda$  is seen to be insignificant in the fully developed region as well.

#### 4.4 Effect of roughness element height on heat transfer

Figure 8 shows the experimental Nu normalized by the theoretical Nu for laminar fully developed flow in a plain channel,  $Nu/Nu_{th,plain}$ , plotted as a function of roughness element height  $H$ . The data sets are for a

roughness element pitch  $\lambda=250 \mu\text{m}$  with two different hydraulic diameters.

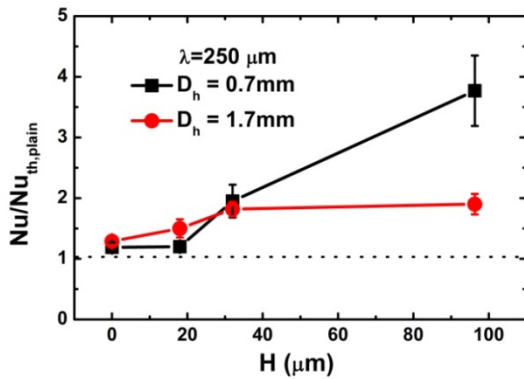


Fig. 8 The effect of roughness element height  $H$  for a roughness elements pitch  $250 \mu\text{m}$

Both data sets exhibit an increase in heat transfer with roughness element height. However, for  $H=96.3 \mu\text{m}$  it is observed that the enhancement for  $D_h=1.7 \text{ mm}$  was significantly lower than that for  $D_h=0.7 \text{ mm}$ . The heat transfer coefficient is thus seen to be dependent on the relative roughness  $H/D_h$  and increases with it. Hence with the same  $H=96.3 \mu\text{m}$ , the enhancement for  $D_h=1.7 \text{ mm}$  is lower than that for  $D_h=0.7 \text{ mm}$ . From Table 1 it is seen that  $H/D_h$  values are 5.1% and 11.1% for a large channel (**B-2**) and a small channel (**B-1**), respectively. The relative roughness of **B-2** ( $H/D_h=5.1\%$ ) is similar to that for channel **C-1** ( $H/D_h=4.3\%$ ). Comparing  $Nu/Nu_{th,plain}$  for these two geometries as shown in Fig. 9, it is seen that the heat transfer enhancement of **C-1** and **B-2** are quite similar. In general, heat transfer enhancement increases with increasing  $H/D_h$  for both channel diameters.

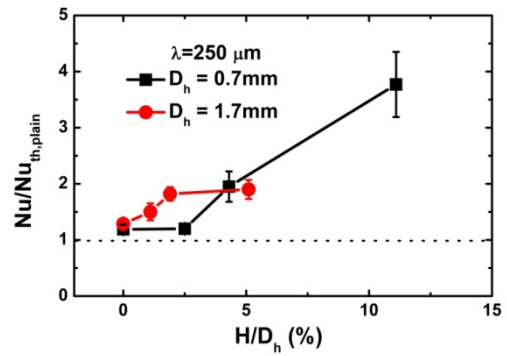


Fig. 9 The effect of relative roughness element height  $H/D_h$  for a roughness elements pitch  $250 \mu\text{m}$

#### 4.5 Early transition from laminar to turbulent flow

Figure 10 shows the  $Nu$  data sets of **B-1**, **B-2** and **C-1** plotted as a function of  $Re$ . The channels with **B-1** and **B-2** have the same roughness elements and different  $D_h$ , while the channels of **B-1** and **C-1** have the same diameter and roughness element pitch  $\lambda$ , but a different roughness element height  $H$ .

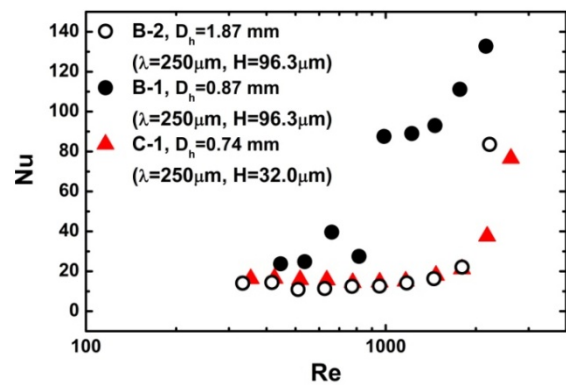


Fig. 10 Comparison of  $Nu$  as a function of  $Re$  for **B-1** ( $\lambda=250$ ,  $H=96.3 \mu\text{m}$ ,  $D_h=0.69 \text{ mm}$ ), **B-2** ( $\lambda=250$ ,  $H=96.3 \mu\text{m}$ ,  $D_h=1.71 \text{ mm}$ ) and **C-1** ( $\lambda=250$ ,  $H=32.0 \mu\text{m}$ ,  $D_h=0.68 \text{ mm}$ )

At lower  $Re$ , the three data sets are weakly dependent on  $Re$ . However, for  $Re > 900$ , the



Nu for **B-1** is significantly enhanced. This is believed to be due to a flow regime transition from laminar to turbulent flow. In turbulent flow, the heat transfer coefficient is much higher than that in laminar flow and Nu increases with Re. Earlier transition from laminar to turbulent flow was observed for **B-1** data sets. The data of **B-2** and **C-1** revealed that the Nu is independent of Re, indicating that no early transition occurred for **B-2** and **C-1**; the transition is seen to occur for these two channels around Re=2,000.

The heat transfer coefficients for **B-1**, **B-2** and **C-1** are shown in Fig. 11. It is observed that h for **C-1** is higher than that for **B-2**, while Nu values for the two channels are similar. This is due to the fact that the diameter of **C-1** is lower than that of **B-2**. Earlier transition was observed only for **B-1**.

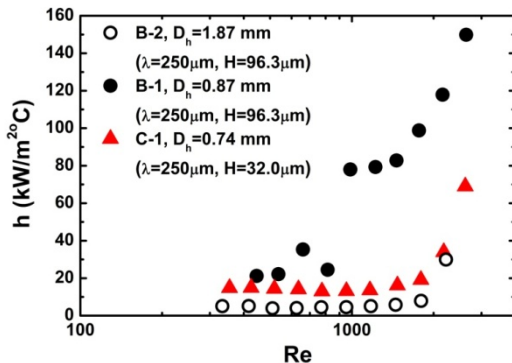


Fig. 11 Comparison of h as a function of Re for **B-1** ( $\lambda=250$ ,  $H=96.3 \mu\text{m}$ ,  $D_h=0.69 \text{ mm}$ ), **B-2** ( $\lambda=250$ ,  $H=96.3 \mu\text{m}$ ,  $D_h=1.71 \text{ mm}$ ) and **C-1** ( $\lambda=250$ ,  $H=32.0 \mu\text{m}$ ,  $D_h=0.68 \text{ mm}$ )

Comparing Figs. 10 and 11, it is concluded that the earlier transition is due to the high value of relative roughness  $H/D_h$ . Brackbill and Kandlikar [38] studied the effect of relative roughness on transition Re, and proposed the following correlation based on

the transition indicated by their friction factor data

$$0 < \frac{H}{D_h} \leq 0.08, \quad Re_t = Re_o - \frac{Re_o - 800}{0.08} 800 \left( \frac{H}{D_h} \right) \quad (12a)$$

$$0.08 < \frac{H}{D_h} \leq 0.25, \quad Re_t = 800 - 3,270 \left( \frac{H}{D_h} - 0.08 \right) \quad (12b)$$

where  $Re_t$  is the transition Reynolds number from laminar to turbulent flow and  $Re_o$  is the transition Reynolds number for a smooth channel with the same geometry and aspect ratio. The calculated transition Re based on  $H/D_h=0.14$  is  $Re_t=604$ . From Figs. 10 and 11 the transition Reynolds number is seen to be around  $Re=900$ . The difference in  $Re_t$  for these two studies may be attributed to the differences in the surface profiles used in the two studies; the smoother profile in the current study yields a higher  $Re_t$ .

The roughness effect on friction factor for the geometries shown in Table 1 are reported from a separate publication by Wagner and Kandlikar [40]. Figure 12 shows friction factors for three surfaces **B-1**, **B-2** and **C-1**. It is seen that the transition from laminar to turbulent flow occurs around  $Re=700$  to  $Re=800$  for these surfaces. The transition Re reported from the friction factor studies is similar to that observed from the heat transfer studies in the present study for **B-1**. Similar observations are made by comparing the friction factor data for **B-2** and **C-1** with the heat transfer data shown in Figs. 10 and 11.

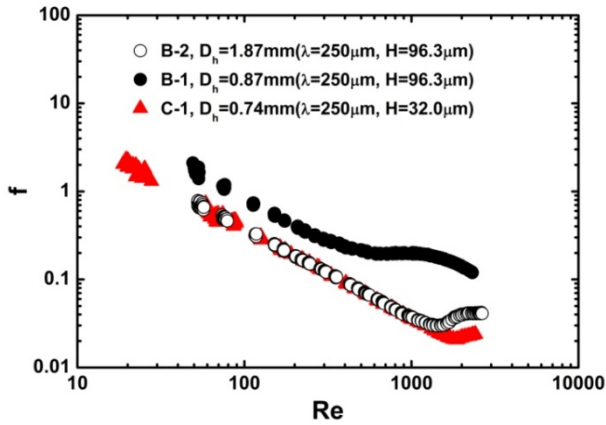


Fig. 12 Comparison of  $f$  as a function of  $Re$  for **B-1** [40] ( $\lambda=250$ ,  $H=96.3 \mu\text{m}$ ,  $D_h=0.69 \text{ mm}$ ), **B-2** ( $\lambda=250$ ,  $H=96.3 \mu\text{m}$ ,  $D_h=1.71 \text{ mm}$ ) and **C-1** ( $\lambda=250$ ,  $H=32.0 \mu\text{m}$ ,  $D_h=0.68 \text{ mm}$ )

It is seen from earlier discussion, that the surface **B-1** performed the best among the different surfaces tested. The friction factor increase and the heat transfer enhancement for the roughness element **B-1** are displayed in Fig. 13 in terms of the  $f$  and  $j$ -factor, which are commonly used in reporting performance data for compact heat exchanger surfaces. The dimensionless heat transfer coefficient  $j$  is defined as:

$$j = StPr^{2/3} \quad (13)$$

It is found that the enhancement in  $f$  and  $j$  are quite similar. Both of the data revealed a slope change between  $Re=700$  and  $Re=900$ , which indicated an earlier transition to turbulent flow. The heat transfer enhancement is generally compared with the friction factor increase when considering their applicability in heat exchangers. The enhancement is measured in terms of a thermal performance index  $\eta$  that compares the heat transfer enhancement to the pumping power requirement and is defined as:

$$\eta = \frac{Nu/Nu_{th,plain}}{(f/f_{th,plain})^{1/3}} \quad (14)$$

The thermal performance index for surface **B-1** is compared with some of the recent enhancement studies reported in the literature [32], [33] and [34] with tape and other inserts in the flow channel.

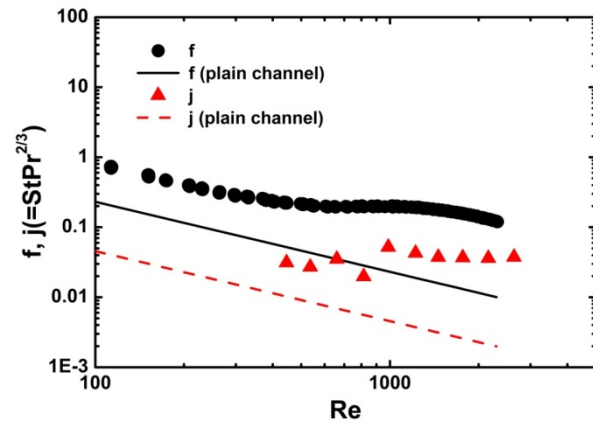


Fig. 13 Comparison of  $f$  and  $j (=StPr^{2/3})$  as a function of  $Re$  for **B-1** ( $\lambda=250$ ,  $H=96.3 \mu\text{m}$ ,  $D_h=0.69 \text{ mm}$ )

Figure 14 shows the results of this comparison, and it can be seen that the performance factor for the surface **B-1** is better than the other surfaces. The heat transfer enhancement  $Nu/Nu_{th,plain}$  reported by Wongcharee and Eisama-ard [33] using alternate clockwise and counter-clockwise twisted tapes is about 6 to 13, but the friction factor increase is about 8 to 15 fold. The heat transfer enhancement  $Nu/Nu_{th,plain}$  reported by Huang et al. [34] with a porous medium insert is about 5.5 to 4.5, but their friction factor enhancement is very high, about 50 to 60 fold. In laminar flow, heat transfer performance was significantly enhanced by inserting twist, porous material, and coiled wires. Similar observations are made by Krishna et al. with the twisted tape inserts in a plain tube with a full twist, and

Akhavan et al. [35] for a coiled insert. From the data in Fig. 14 it is seen that by generating internal roughness structure on microchannels the heat transfer coefficient is efficiently enhanced.

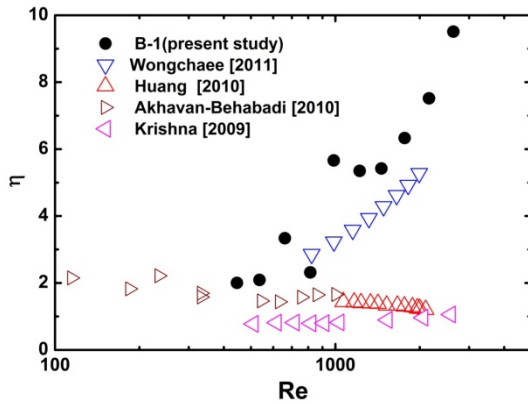


Fig. 14 Comparison of  $\eta$  of **B-1** ( $\lambda=250$ ,  $H=96.3 \mu\text{m}$ ,  $D_h=0.69 \text{ mm}$ ) to available data in recent literature [32-35]

## 5. Discussions

From the experimental data reported in this investigation, it was found that structured roughness enhanced the heat transfer. The Nu data from fully developed laminar flow in 8 rough channels, and the friction factor data in [40], are summarized in Table 2. For all rough channels, heat transfer was enhanced and  $Nu/Nu_{th,plain}$  are all found to be greater than 1. The enhancement was normalized with respect to the plain tube results.

Although heat transfer enhancement of **B-1** is as high as 377%, which is significantly higher than the other channels, it should be noted that the enhancement of the friction factor is 371%, which is also significantly higher than the other channels. From the summary of Nu and f data in the present study and [40], it was found that heat transfer enhancement due to

roughness is higher than the friction factor in the parametric ranges investigated. The simulation work of Dharaiya and Kandlikar [44] indicated that the laminar fully developed Nu for the same roughness structure is 30.7 which is very close to the experimental Nu 28.9 in the present study; there is only a 6% difference between the simulated results and the experimental data.

Table 2 Heat transfer and friction factor enhancement of rough channels

Channel	B-1	B-2	C-1	C-2	D-1	D-2	E-1	E-2
Nu	28.9	13.4	15.1	13	14.4	14	9.3	10.7
$Nu_{th,plain}$	7.67	7.05	7.75	7.16	7.73	7.08	7.77	7.15
$Nu/Nu_{th,plain}$	3.77	1.9	1.95	1.82	1.87	1.98	1.2	1.5
f	83.7	37.6	37.6	26.7	28.7	23.7	26.1	25.3
$f_{th,plain}$	23.1	21.9	23.1	22.2	23.1	22.2	23.1	22.5
$f/f_{th,plain}$	3.71	1.65	1.59	1.22	1.28	1.03	1.14	1.09
$\eta$	2.44	1.61	1.67	1.7	1.72	1.96	1.15	1.46

Coleman et al. (2007) [45] experimentally and numerically assessed the effect of transverse rib roughness pitch-to-height ratios,  $\lambda/H$ , on turbulent flow. The maximum drag was reported to be at  $\lambda/H$  around 8. The authors reported a smooth transition from skimming flow to interactive flow at a rib spacing of  $\lambda/H = 5$ . In the extremes where  $\lambda/H$  is significantly greater than 5, or less than 5, the roughness effect is expected to diminish. Although these publications discussing roughness ratios focus on turbulent flows, the concept may still hold true for microscale laminar flows. Webb et al. [46] revealed flow patterns over transverse-rib roughness as a function of rib spacing. The flow separates at the rib and reattaches six-to-eight rib heights downstream from the rib. The reattachment does not occur for  $\lambda/H$  less than 8.

The heat transfer coefficient attains the maximum values near the attachment point; the highest enhancement occurs for  $\lambda/H$  between 10 to 15.

To study the effect of pitch to height ratio, the heat transfer and friction factor enhancement is plotted as a function of  $\lambda/H$  in Fig. 15. It is found that the enhancement decreases with the increasing of  $\lambda/H$ . Pethkool et al. [47] investigated heat transfer enhancement in a helically corrugated tube. Their data showed that the effect of relative roughness was higher than the effect of pitch. Figure 16 shows the effect of relative roughness on the enhancements. Both heat transfer and friction factor enhancements increase with increasing  $H/D_h$ . Further experiments are needed to cover the wider ranges of pitch to height ratio, although the trends observed in the present work are in agreement with the effects seen for other similar geometries by earlier investigators.

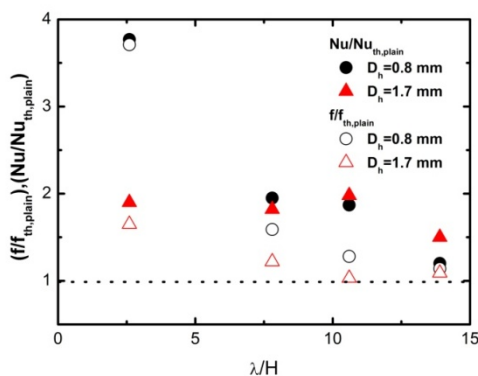


Fig. 15.  $f$  and  $Nu$  enhancement ratio of as a function of  $\lambda/H$

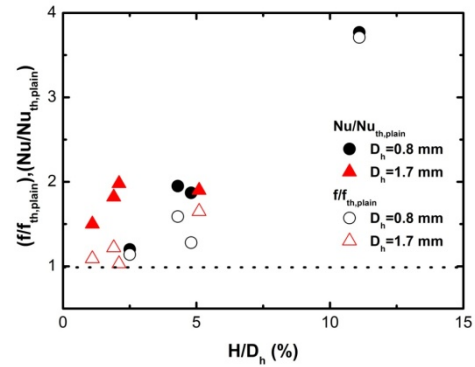


Fig. 16.  $f$  and  $Nu$  enhancement ratio of as a function of  $H/D_h$

## 6 Conclusions

The heat transfer performance of water flowing in smooth channels and channels with structured roughness surfaces was experimentally investigated in the present study. The following conclusions are drawn based on the experimental results:

1. The experimental data of smooth channels indicated that the  $Nu$  agrees well with conventional correlation predictions in both developing and fully developed flows.
2. The heat transfer coefficient was found to be significantly enhanced by roughness structure. Surfaces with higher  $H/D_h$  had large enhancement in both heat transfer and pressure drop.
3. The roughness element pitch did not affect heat transfer significantly in the range investigated.
4. Relative roughness  $H/D_h$  has a more significant effect on heat transfer than  $H$ .
5. The thermal performance index for roughness structure with a high relative roughness was found to be at least comparable to the tape and coil inserts examined by earlier investigators.
6. An earlier transition from laminar to turbulent flow was observed in high  $H/D_h$

rough channels, and the transition Reynolds number obtained from heat transfer studies corresponded with the transition noted from the friction factor data. The transition Reynolds numbers were in reasonable agreement with the transition models based on relative roughness proposed by Brackbill and Kandlikar [38], although the smoother profile in the present study seems to have delayed the transition.

## Nomenclature

a	Channel height, m
$A_h$	Flow heat transfer area, $m^2$
$A_{h,s}$	Cross-section area of channel, $m^2$
$A_f$	Cross-section area of fluid flow in channel, $m^2$
b	Channel width, m
$c_p$	Heat capacity, $J/kg\ ^\circ C$
$D_h$	Hydraulic diameter, m
f	Friction factor, dimensionless
$f_{th,plain}$	Theoretical friction factor for smooth channel, dimensionless
Gz	Graetz number, dimensionless
h	Heat transfer coefficient, $W/m^2\ ^\circ C$
$h_x$	Local heat transfer coefficient, $W/m^2\ ^\circ C$
H	Roughness elements height, m
I	Current, A
$k_s$	Wall thermal conductivity, $W/m\ ^\circ C$
$k_f$	Fluid thermal conductivity, $W/m\ ^\circ C$
$k_{f,x}$	Local fluid thermal conductivity, $W/m\ ^\circ C$
$L_{h,x}$	Local heating location distance from the entrance, m
$L_{h,All}$	Total heating length of channel, m
$\dot{m}$	Mass flow rate, kg/s
Nu	Nusselt number, dimensionless
$Nu_{k0}$	Nusselt number without axial conduction, dimensionless
$Nu_{th,plain}$	Nusselt number for plain channel in developing flow, dimensionless
$Nu_x$	Local Nusselt number, dimensionless
Pr	Prandtl number, dimensionless
$q_{conv}$	Input power to the fluid, W
$q_{mea}$	Measured input power, W
$q_{loss}$	Heat loss, W
$q''_{avg}$	Average heat flux, $W/m^2$
Re	Reynolds number, dimensionless

$Re_t$	Transition Reynolds number, dimensionless
$Re_o$	Transition Reynolds number for smooth channel, dimensionless
$T_{f,i}$	Channel inlet fluid temperature, $^\circ C$
$T_{f,o}$	Channel outlet fluid temperature, $^\circ C$
$T_{f,x}$	Local fluid temperature, $^\circ C$
$T_{w,x}$	Local wall temperature, $^\circ C$
V	Voltage, V

## Greek symbols

$\alpha$	Aspect ratio a/b, m
$\eta$	Performance factor, dimensionless
$\lambda$	Roughness elements pitch, m

## References

- [1] Wu, P., and Little, W. A., 1984, "Measurement of the Heat Transfer Characteristics of Gas Flow in Fine Channel Heat Exchangers Used for Microminiature Refrigerators," *Cryogenics*, 24(8), pp. 415-420.
- [2] Peng, X. F., and Wang, B. X., 1993, "Forced convection and flow boiling heat transfer for liquid flowing through microchannels," *International Journal of Heat and Mass Transfer*, 36(14), pp. 3421-3427.
- [3] Wang, B. X., and Peng, X. F., 1994, "Experimental investigation on liquid forced-convection heat transfer through microchannels," *International Journal of Heat and Mass Transfer*, 37, pp. 73-82.
- [4] Peng, X. F., and Peterson, G. P., 1995, "Effect of thermofluid and geometrical parameters on convection of liquids through rectangular microchannels," *International Journal of Heat and Mass Transfer*, 38(4), pp. 755-758.
- [5] Peng, X. F., and Peterson, G. P., 1996, "Convective heat transfer and flow friction for water flow in microchannel structures," *International Journal of Heat and Mass*

Transfer, 39(12), pp. 2599-2608.

[6] Qu, W., Mala, G. M., and Li, D., 2000, "Heat transfer for water flow in trapezoidal silicon microchannels," *International Journal of Heat and Mass Transfer*, 43(21), pp. 3925-3936.

[7] Lin, T.-Y., and Yang, C.-Y., 2007, "An experimental investigation on forced convection heat transfer performance in micro tubes by the method of liquid crystal thermography," *International Journal of Heat and Mass Transfer*, 50(23-24), pp. 4736-4742.

[8] Yang, C. Y., and Lin, T. Y., 2007, "Heat transfer characteristics of water flow in microtubes," *Experimental Thermal and Fluid Science*, 32(2), pp. 432-439.

[9] Lelea, D., Nishio, S., and Takano, K., 2004, "The experimental research on microtube heat transfer and fluid flow of distilled water," *International Journal of Heat and Mass Transfer*, 47(12-13), pp. 2817-2830.

[10] Steinke, M. E., and Kandlikar, S. G., 2006, "Single-phase liquid friction factors in microchannels," *International Journal of Thermal Sciences*, 45, pp. 1073-1083.

[11] Guo, Z.-Y., and Li, Z.-X., 2003, "Size effect on microscale single-phase flow and heat transfer," *International Journal of Heat and Mass Transfer*, 46, pp. 149-159.

[12] Guo, Z.-Y., and Li, Z.-X., 2003, "Size effect on single-phase channel flow and heat transfer at microscale," *International Journal of Heat and Fluid Flow*, 24, pp. 284-298.

[13] Morini, G. L., 2004, "Single-phase convective heat transfer in microchannels: A review of experimental results," *International Journal of Thermal Sciences*, 43(7), pp. 631-651.

[14] Rostami, A. A., Mujumdar, A. S., and Saniei, N., 2002, "Flow and heat transfer for gas flowing in microchannels: A review," *Heat and Mass Transfer/Waerme- und Stoffuebertragung*, 38(4-5), pp. 359-367.

[15] Rosa, P., Karayiannis, T. G., and Collins, M. W., 2009, "Single-phase heat transfer in microchannels: the importance of scaling effects," *Applied Thermal Engineering*, 29, pp. 3447-3468.

[16] Hetsroni, G., Mosyak, A., Pogrebnyak, E., and Yarin, L. P., 2005, "Heat transfer in micro-channels: Comparison of experiments with theory and numerical results," *International Journal of Heat and Mass Transfer*, 48, pp. 5580-5601.

[17] Celata, G. P., Cumo, M., and Zummo, G., 2004, "Thermal-hydraulic characteristics of single-phase flow in capillary pipes," *Experimental Thermal and Fluid Science*, 28(2-3), pp. 87-95.

[18] Li, Z.-X., Du, D.-X., and Guo, Z.-Y., 2003, "Experimental study on flow characteristics of liquid in circular microtubes," *Microscale Thermophysical Engineering*, 7(3), pp. 253-265.

[19] Mala, G. M., and Li, D., 1999, "Flow characteristics of water in microtubes," *International Journal of Heat and Fluid Flow*, 20, pp. 142-148.

[20] Herwig, H., and Hausner, O., 2003, "Critical view on "new results in micro-fluid mechanics": An example," *International Journal of Heat and Mass Transfer*, 46, pp. 935-937.

[21] Tso, C. P., and Mahulikar, S. P., 2000, "Experimental verification of the role of Brinkman number in microchannels using

local parameters," *International Journal of Heat and Mass Transfer*, 43, pp. 1837-1849.

[22] Cheng, P., and Wu, H. Y., 2003, "An experimental study of convective heat transfer in silicon microchannels with different surface conditions," *International Journal of Heat and Mass Transfer*, 46(14), pp. 2547-2556.

[23] Shen, S., Xu, J. L., Zhou, J. J., and Chen, Y., 2006, "Flow and heat transfer in microchannels with rough wall surface," *Energy Conversion and Management*, 47(11-12), pp. 1311-1325.

[24] Tiselj, I., Hetsroni, G., Mavko, B., Mosyak, A., Pogrebnyak, E., and Segal, Z., 2004, "Effect of axial conduction on the heat transfer in micro-channels," *International Journal of Heat and Mass Transfer*, 47, pp. 2551-2565.

[25] Lin, T. Y., Kandlikar, S. G., 2011, "A Theoretical Model for Axial Heat Conduction Effects During Single-Phase Flow in Microchannels," Submitted to *Journal of Heat Transfer*.

[26] Rahman, M. M., 2000, "Measurements of heat transfer in microchannel heat sinks," *International Communications in Heat and Mass Transfer*, 27(4), pp. 495-506.

[27] Wu, H. Y., and Cheng, P., 2003, "An experimental study of convective heat transfer in silicon microchannels with different surface conditions," *International Journal of Heat and Mass Transfer*, 46, pp. 2547-2556.

[28] Kandlikar, S. G., Joshi, S., and Tian, S., 2003, "Effect of surface roughness on heat transfer and fluid flow characteristics at low Reynolds numbers in small diameter tubes," *Heat Transfer Engineering*, 24(3), pp. 4-16.

[29] Shen, S., Xu, J. L., Zhou, J. J., and Chen,

Y., 2006, "Flow and heat transfer in microchannels with rough wall surface," *Energy Conversion and Management*, 47, pp. 1311-1325.

[30] Grohmann, S., 2005, "Measurement and modeling of single-phase and flow-boiling heat transfer in microtubes," *International Journal of Heat and Mass Transfer*, 48(19-20), pp. 4073-4089.

[31] Webb, R. L., 1992, "Principles of enhanced heat transfer," John Wiley & Sons, New York.

[32] Krishna, S. R., Pathipaka, G., and Sivashanmugam, P., 2009, "Heat transfer and pressure drop studies in a circular tube fitted with straight full twist," *Experimental Thermal and Fluid Science*, 33, pp. 431-438.

[33] Wongcharee, K., and Eiamsa-ard, S., 2011, "Friction and heat transfer characteristics of laminar swirl flow through the round tubes inserted with alternate clockwise and counter-clockwise twisted-tapes," *International Communications in Heat and Mass Transfer*, 38, pp. 348-352.

[34] Huang, Z. F., Nakayama, A., Yang, K., Yang, C., and Liu, W., 2010, "Enhancing heat transfer in the core flow by using porous medium insert in a tube," *International Journal of Heat and Mass Transfer*, 53, pp. 1164-1174.

[35] Akhavan-Behabadi, M. A., Kumar, R., Salimpour, M. R., and Azimi, R., 2010, "Pressure drop and heat transfer augmentation due to coiled wire inserts during laminar flow of oil inside a horizontal tube," *International Journal of Thermal Sciences*, 49, pp. 373-379.

[36] Kandlikar, S. G., 2005, "Roughness effects at microscale - Reassessing Nikuradse's experiments on liquid flow in rough tubes,"

Bulletin of the Polish Academy of Sciences: Technical Sciences, 53(4), pp. 343-349.

[37] Brackbill, T. P., and Kandlikar, S. G., 2007, "Effect of sawtooth roughness on pressure drop and turbulent transition in microchannels," *Heat Transfer Engineering*, 28(8-9), pp. 662-669.

[38] Brackbill, T. P., and Kandlikar, S. G., 2010, "Application of lubrication theory and study of roughness pitch during laminar, transition, and low reynolds number turbulent flow at microscale," *Heat Transfer Engineering*, 31(8), pp. 635-645.

[39] Kandlikar, S. G., Schmitt, D., Carrano, A. L., and Taylor, J. B., 2005, "Characterization of surface roughness effects on pressure drop in single-phase flow in minichannels," *Physics of Fluids*, 17(10), p. 100606.

[40] Wagner, R. N., and Kandlikar, S. G., "Effects of structured roughness on fluid flow at the microscale level," Submitted to *International Journal of Heat and Fluid Flow*.

[41] Maranzana, G., Perry, I., and Maillet, D., 2004, "Mini- and micro-channels: Influence of axial conduction in the walls," *International Journal of Heat and Mass Transfer*, 47(17-18), pp. 3993-4004.

[42] Harms, T. M., Kazmierczak, M. J., and Gerner, F. M., 1999, "Developing convective heat transfer in deep rectangular microchannels," *International Journal of Heat and Fluid Flow*, 20, pp. 149-157.

[43] Amon, C. H., and Mikic, B. B., 1991, "Spectral element simulations of unsteady forced convective heat transfer: application to compact heat exchanger geometries," *Numerical Heat Transfer, Part A (Applications)*, 19, pp. 1-19.

[44] Dharaiya, V. V., and Kandlikar, S. G., 2011, "A Numerical Study to Predict the Effects of Structured Roughness Elements on Pressure Drop and Heat Transfer Enhancement in Minichannels and Microchannels," ASME 2011 International Mechanical Engineering Congress & Exposition Denver, Colorado.

[45] Coleman, S. E., Nikora, V. I., McLean, S. R., and Schlicke, E., 2007, "Spatially averaged turbulent flow over square ribs," *Journal of Engineering Mechanics*, 133, pp. 194-204.

[46] Webb, R. L., Eckert, E. R. G., and Goldstein, R. J., 1971, "Heat transfer and friction in tubes with repeated- rib roughness," *International Journal of Heat and Mass Transfer*, 14, pp. 601-617.

[47] Pethkool, S., Eiamsa-ard, S., Kwankaomeng, S., and Promvonge, P., 2011, "Turbulent heat transfer enhancement in a heat exchanger using helically corrugated tube," *International Communications in Heat and Mass Transfer*, 38, pp. 340-347.